◆ Human Brain Mapping 34:3129–3142 (2013) ◆

Loss in Connectivity Among Regions of the Brain Reward System in Alcohol Dependence

Amy Kuceyeski,[1]* Dieter J. Meyerhoff,[2,3] Timothy C. Durazzo,[2,3] and Ashish Raj[1]

[1]*Imaging Data Evaluation and Analytics Laboratory (IDEAL), Department of Radiology, Weill Cornell Medical College, New York, New York*
[2]*Department of Radiology and Biomedical Imaging, University of California San Francisco, San Francisco, California*
[3]*Center for Imaging of Neurodegenerative Diseases, San Francisco Veterans Administration Medical Center, San Francisco, California*

Abstract: A recently developed measure of structural brain connectivity disruption, the loss in connectivity (LoCo), is adapted for studies in alcohol dependence. LoCo uses independent tractography information from young healthy controls to project the location of white matter (WM) microstructure abnormalities in alcohol-dependent versus nondependent individuals onto connected gray matter (GM) regions. LoCo scores are computed from WM abnormality masks derived at two levels: (1) groupwise differences of alcohol-dependent individuals (ALC) versus light-drinking (LD) controls and (2) differences of each ALC individual versus the LD control group. LoCo scores based on groupwise WM differences show that GM regions belonging to the extended brain reward system (BRS) network have significantly higher LoCo (i.e., disconnectivity) than those not in this network ($t = 2.18$, $P = 0.016$). LoCo scores based on individuals' WM differences are also higher in BRS versus non-BRS ($t = 5.26$, $P = 3.92 \times 10^{-6}$) of ALC. These results suggest that WM alterations in alcohol dependence, although subtle and spatially heterogeneous across the population, are nonetheless preferentially localized to the BRS. LoCo is shown to provide a more sensitive estimate of GM involvement than conventional volumetric GM measures by better differentiating between brains of ALC and LD controls (rates of 89.3% vs. 69.6%). However, just as volumetric measures, LoCo is not significantly correlated with standard metrics of drinking severity. LoCo is a sensitive WM measure of regional cortical disconnectivity that uniquely characterizes anatomical network disruptions in alcohol dependence. *Hum Brain Mapp 34:3129–3142, 2013.* © 2012 Wiley Periodicals, Inc.

Key words: structural brain connectivity; tractography; white matter injury; alcohol dependence; addiction; brain reward system

Additional Supporting Information may be found in the online version of this article.

Contract grant sponsor: National Institutes of Health; Contract grant numbers: F32 EB012404-02 (A.K.), P41 EB0159504 (A.R. and D.J.M.), P41 RR023953-02S1 (A.R.), R21 EB008138-02 (A.R.), AA10788 (D.J.M.), R01 AA10788 (D.J.M), K01 DA24136 (T.C.D.), DA24136 (T.C.D.); Contract grant sponsor: Radiology Research Service of the San Francisco Veteran's Administration Medical Center

*Correspondence to: Amy Kuceyeski, 515 E. 71st St., New York, NY 10044. E-mail: amk2012@med.cornell.edu

Received for publication 10 November 2011; Revised 5 April 2012; Accepted 26 April 2012

DOI: 10.1002/hbm.22132

Published online 19 July 2012 in Wiley Online Library (wileyonlinelibrary.com).

INTRODUCTION

Over the past two decades, many different in vivo magnetic resonance imaging (MRI) techniques have been used to assess the effects of alcohol and substance use disorders on human brain morphology. Widely applied quantitative methods include voxel-based morphometry, deformation-based morphometry, region of interest (ROI) analyses of cortical volume [for review, see Durazzo and Meyerhoff, 2007], and more recently, cortical surface area and thickness [Durazzo et al., 2011]. A primary limitation of most of these methods is that they are specific to cortical and subcortical gray matter (GM) and do not permit assessment of the integrity of white matter (WM). Human neurocognition, emotion, and motor functions, however, are largely subserved by complex circuits formed by myelinated association, projection, and commissural fibers that interconnect various cortical and subcortical regions [Filley, 2005; Kolb et al., 2009]. Additionally, increasing evidence suggests that the development and maintenance of alcohol and other substance use disorders are related to neurobiological abnormalities in corticocortical and corticosubcortical circuits that mediate reward-related processes and behaviors [Koob and Volkow, 2010; Volkow et al., 2010]. Therefore, interrogation of the microstructural integrity of WM fiber networks that form the interconnectivity among brain regions involved in reward-related behavior is critical to understand the mechanisms contributing to the maintenance of these disorders and associated neurocognitive, psychiatric, and psychosocial dysfunctions.

Microstructural integrity of fiber networks that comprise WM is accurately and sensitively captured by diffusion-weighted MRI through the quantitation of water diffusion in fiber tracts [for application to alcohol dependence see, e.g., Pfefferbaum et al., 2005 and Sullivan et al., 2005]. The morphology of WM tracts demonstrates a consistent structure and orientation, which restricts the diffusion and the direction of water movement. Fractional anisotropy (FA) is a diffusion tensor imaging (DTI) metric that quantitates the degree of anisotropy in water diffusion in an image voxel. Reduced FA has been associated with degradation of both myelin sheaths and axonal membranes [Pierpaoli et al., 2001; Werring et al., 2000], abnormalities of myelin with sparing of the axonal fibers [Gulani et al., 2001; Song et al., 2002], or reduced density of axonal fibers [Takahashi et al., 2002]. An increasing number of studies suggest that abnormalities in FA are apparent before volumetric deficits in conditions associated with neurodegeneration, including Alzheimer's disease and alcohol use disorders [Bendlin et al., 2010; Gold et al., 2010; Smith et al., 2010; Sullivan et al., 2005; Yeh et al., 2009]. Data from alcohol-dependent individuals suggest adverse microstructural changes in WM regions that include major association and commissural fiber tracts in the frontal lobe, mesial temporal lobe, and corticostriatal regions [Pfefferbaum et al., 2005; Yeh et al., 2009]. Abnormal regional DTI measures have been related to cognitive deficiencies and severity of alcohol consumption, thus suggesting a dose-dependent, functionally significant compromise in the integrity of WM microstructure as a prominent neurobiological abnormality associated with alcohol dependence [Pfefferbaum et al., 2006, 2007; Sullivan et al., 2010; Yeh et al., 2009].

In this study, we exploit the sensitivity of diffusion-based measurements in the WM to inform and estimate concomitant changes occurring in the connectivity of GM regions in abstinent alcohol-dependent individuals (ALC). Although many cortical and subcortical brain regions are intimately related via WM fiber tracts [Aralasmak et al., 2006; Schmahmann et al., 2007], WM and/or GM changes in these regions neither do necessarily occur at the same time or on the same time scale, nor do the imaging modalities that track such changes have the same sensitivity. Therefore, we postulate that by using whole brain tractography information and the location of alcohol-dependent WM abnormalities, we can estimate the degree of anatomical connectivity disruption for each cortical region.

We implement a recently developed measure of GM integrity called loss in connectivity (LoCo) by following the WM fiber tracts passing through regions of significant WM integrity loss (relative to controls) to their terminating GM regions. Specifically, we define LoCo of a GM region as the proportion of fiber tracts out of the total number of tracts terminating in that region that pass through identified damaged WM loci. In a previous study [Kuceyeski and Raj, 2011; Kuceyeski et al., 2012], we showed that LoCo is an excellent biomarker of Alzheimer's disease and frontotemporal dementia, and we found it significantly correlated with corresponding GM atrophy. In addition to LoCo, the proposed approach provides whole brain connectivity networks and measures how global metrics on these networks change under conditions associated with WM abnormalities. Connectivity networks have been increasingly applied to assess macroscopic structural and functional brain differences in, for example, schizophrenia [Zalesky et al., 2010], healthy aging [Wen et al., 2011], Alzheimer's disease [Lo et al., 2010], and traumatic brain injury [Kuceyeski et al., 2011].

Application to Alcohol Use Disorders

We apply the proposed analytic methods to abstinent ALC and non/light-drinking (LD) controls. Long-term chronic alcohol consumption, often accompanied by chronic cigarette smoking [Durazzo and Meyerhoff, 2007], is associated with macrostructural and microstructural abnormalities in cortical and subcortical GM and WM [Sullivan, 2007; Sullivan et al., 2005]. The most prominent abnormalities in alcohol use disorders are observed in anterior frontal neocortical and paralimbic GM and WM, diencephalon, limbic structures, and the cerebellum [Durazzo and Meyerhoff, 2007]. In this study, we focus on anatomical regions that comprise the extended brain reward system (BRS). Accumulating evidence from neuroscience research strongly suggests that neurobiological abnormalities of the BRS underlie

TABLE I. ALC and LD demographic information

Variables	Alcohol dependent ($N = 35$)	Controls ($N = 21$)
Age (years)	53.1 (8.4)	50.5 (9.3)
Education (years)	13.9 (1.9)	15.5 (2.4)
Caucasian (%)	71	57
AMNART	113 (19)	119 (5)
One year average drinks (month)	360 (172)	18 (21)
Lifetime average drinks (month)	214 (118)	19 (13)
Lifetime (years)	36 (9)	28 (9)
Lifetime alcohol consumption	1,242 (735)	92 (82)
Months heavy drinking	275 (111)	N/A
Onset heavy drinking	25 (8)	N/A
Smokers (%)	66	57
FTND	4 (2)	5 (1)
Total cigarettes per day	16 (8)	18 (5)
Years smoking at current level	18 (12)	27 (12)

AMNART, American National Adult Reading Test; FTND, Fagerstrom Test for Nicotine Dependence; N/A, not applicable, Mean (standard deviation).

development and persistence of alcohol use and other addictive disorders [Durazzo et al., 2011; Durazzo et al., in press and references therein]. The BRS is a collection of discrete and overlapping cortical–subcortical circuits, largely involving anterior frontal, mesial temporal, limbic, striatal, and thalamic subregions, which interact to form the biological substrate for reward/saliency, motivation/drive, conditioning/habits, and inhibitory control/executive function [George et al., 2010; Koob and Volkow, 2010; Volkow et al., 2011]. Here, we apply the proposed LoCo and graph-theoretic metrics to interrogate the integrity of WM fiber networks in ALC in the early phase of recovery from alcohol dependence, when macrostructural changes are relatively prominent and have had little time to normalize during extended abstinence.

We test three main hypotheses:

1. Whole brain graph metrics of anatomical connectivity networks are different between ALC and LD groups.
2. LoCo provides a more sensitive biomarker for alcohol dependence than conventional measures of cortical differences such as volume.
3. The severity of network connectivity disruption as measured by LoCo correlates with measures of drinking severity.

MATERIALS AND METHODS

Participants

Longitudinal studies at the University of California, San Francisco, of the neurobiological and neurocognitive consequences of alcohol use disorders and chronic cigarette smoking provided data from 35 (32 males, three females, 53.1 ± 8.4 years) ALC from outpatient treatment programs in the San Francisco city area (see Table I for demographics).The ALC participants were abstinent for an average of 25 ± 12 days (range 6–42). All ALC participants met diagnostic and statistical manual of mental disorders-IV (DSM-IV) criteria for alcohol dependence at the time of study, according to the structured clinical interview for DSM-IV Axis I Disorder Patient Edition, Version 2.0 [First et al., 1998], performed within 3 days of the MRI session. Inclusion and exclusion criteria are fully detailed in [Durazzo et al., 2004]. Briefly, participants were excluded for a history of abuse or dependence on other substances within the past 5 years (other than nicotine) and for neurological or psychiatric disorders that are known to affect neurobiology or neurocognition. ALC participants consumed more than 150 alcoholic drinks (defined as containing 13.6 g of pure ethanol) per month for at least 8 years (males) or more than 80 drinks per month for at least 6 years (females) before the enrollment. Alcohol consumption was assessed with the lifetime drinking history (LDH) [Skinner and Sheu, 1982; Sobell and Sobell, 1990; Sobell et al., 1988]. From the LDH, we estimated the average number of alcoholic drinks consumed per month over 1 year and over lifetime, number of years of regular (defined as drinking more than one alcoholic drink/month), and heavy drinking (>100 alcoholic drinks/month) as well as age at onset of heavy drinking. Twenty-one age-matched LD controls (all males, 50.5 ± 9.3 years) were recruited from the local community and had no history of medical (except nicotine dependence) or psychiatric conditions known to influence the outcome measures of this study [Durazzo et al., 2004].

A third study group consisted of 14 healthy young participants (nine males, five females, 23.1 ± 4.7 years), whose MRI data were collected jointly by Weill Cornell Medical College and the Brain Trauma Foundation (from here on referred to as "atlas" data). The exclusion criteria for these participants were pregnancy, a history of neurological or psychiatric diagnosis, seizure, or drug or alcohol abuse. This dataset provided high-quality control tractograms and normal, healthy connectivity information (see Image Processing section) that could not have been derived using the ALC and LD datasets. The diffusion data from the ALC and LD groups did not have sufficient spatial resolution or a large enough number of diffusion encoding directions to derive satisfactory tractography information.

Data

MRI data on ALC and LD were acquired on a 4-Tesla Bruker MedSpec system with a Siemens Trio console (Siemens, Erlangen, Germany) using an eight-channel transmit-receive head coil. The structural scan was a three-dimensional (3D)-sagittal magnetization prepared rapid gradient sequence (echo time (TE) of 3 ms, repetition time (TR) of 2,300 ms, inversion time (TI) of 950 ms, flip angle of 7°) with a 256 × 256 matrix over a 256-mm^2 field of view (FOV) and 176 1.0-mm contiguous partitions (final voxel size 1.0 × 1.0 × 1.0 mm^3). The diffusion-weighted

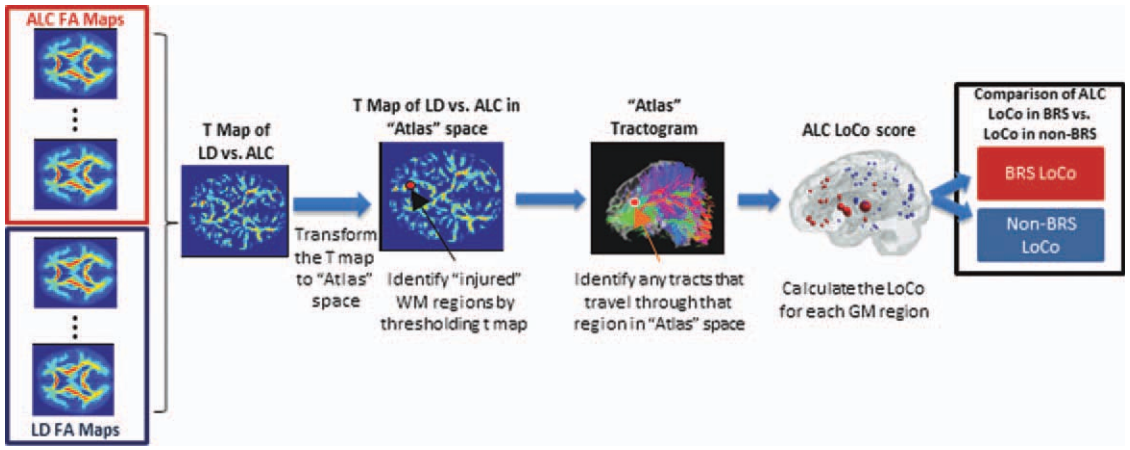

Figure 1.

Pipeline process for calculating LoCo scores using "atlas" tractograms from a healthy young control group and *t*-maps from ALC versus LD FA measures. [Color figure can be viewed in the online issue, which is available at wileyonlinelibrary.com.]

data were acquired with a dual spin echo planar image (EPI) sequence that used six diffusion-encoding directions at $b = 800$ s/mm^2 and one at $b = 0$ s/mm^2 and acquired from 40 3.0-mm thick interleaved slices (no slice gap) and 128 × 112 matrix size, zero-filled during reconstruction to 256 × 256, with a FOV of 256 × 224 mm^2 (final voxel size 2.0 × 2.0 × 3.0 mm^3). Twofold parallel imaging acceleration was used to reduce geometrical distortions [Griswold et al., 2002], and four scans were averaged to boost signal to noise.

T_1-weighted structural and diffusion weighted images on the "atlas" group were collected on a 3-Tesla GE Signa EXCITE scanner (GE Healthcare, Waukesha, WI). The high angular resolution diffusion image data were acquired with 55 isotropically distributed diffusion-encoding directions at $b = 1{,}000$ s/mm^2 and one at $b = 0$ s/mm^2 and acquired from 72 1.8-mm thick interleaved slices (no slice gap) and 128 × 128 matrix size, zero-filled during reconstruction to 256 × 256, with a FOV of 230 mm^2 (final voxel size 0.89 × 0.89 × 1.8 mm^3). The structural scan was an axial 3D inversion recovery fast spoiled gradient-recalled echo sequence (TE = 1.5 ms, TR = 6.3 ms, TI = 400 ms, flip angle of 15°) with a 256 × 256 matrix over a 230 mm^2 FOV and 156 1.0-mm contiguous partitions (final voxel size: 0.89 × 0.89 × 1.0 mm^3).

Image Processing

T1 images for ALC and LD groups were normalized to Montreal Neurological Institute space using the normalize function within statistical parametric mapping [SPM; Friston et al., 2007], a software package within Matlab R2009a (The Mathworks, Natick, MA). The same transformation was subsequently applied to the FA maps. A study specific FA template was found by calculating the mean of the LD group's normalized FA maps, and then each individual's FA map in the ALC and LD was renormalized to it. This two-step process of coregistration helps reduce errors that are common when matching an individual's images to a template.

The "atlas" T1 images were first segmented into 90 different GM regions (the 116 region Automated Anatomical Atlas, minus the cerebellum) using the Individual-Based Atlas toolbox [Alemán-Gómez et al., 2005] within SPM. To obtain normative brain network connectivity information between the 90-parcellated GM regions, probabilistic tractography was performed using the diffusion-weighted MRI. A flow chart of the processing procedures is given in Supporting Information Figure S1; the details of the image processing and tractography methods for the "atlas" images are given in Kuceyeski et al., 2011.

Cortical regions of the BRS were defined a priori based on previous research on the BRS in alcohol and substance use disorders [Cardenas et al., 2011; Durazzo et al., 2010, 2011; Heinz et al., 2009; Makris et al., 2008a, 2008b; Rando et al., 2011]. The following BRS regions of interest were formed from the listed parcellations: dorsolateral prefrontal cortex (superior frontal, rostral, and caudal middle frontal, pars opercularis, and triangularis), anterior cingulate cortex (rostral and caudal), orbitofrontal cortex (medial and lateral), and insula. The following subcortical regions were also identified as components of the BRS: caudate nucleus, putamen, globus pallidus, thalamus, hippocampus, and amygdala.

LoCo Calculation

LoCo was calculated for each of the 90 GM regions via the following process, outlined in Figure 1:

1. The *t*-map of the FA measurements for ALC versus LD were calculated on a voxelwise basis. This *t*-map

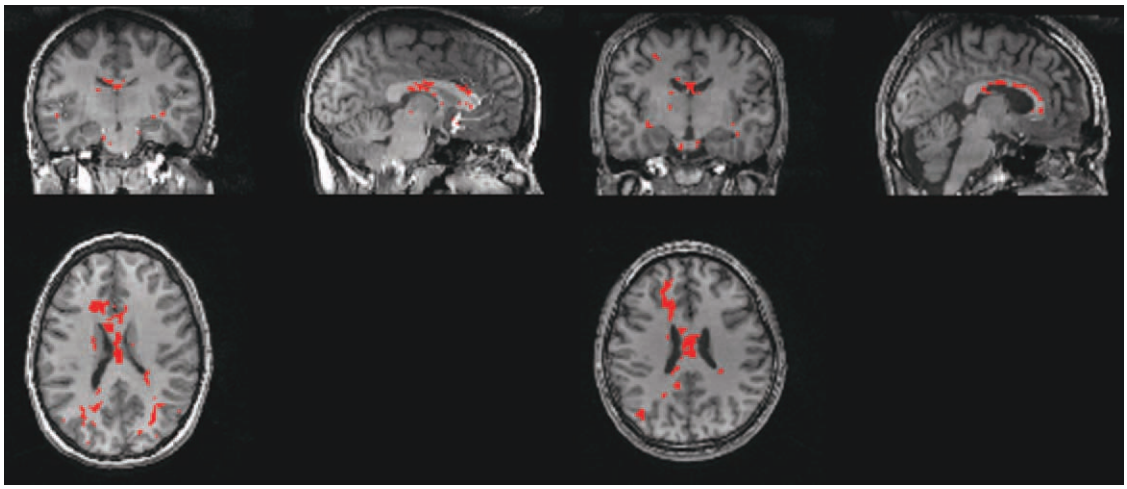

Figure 2.
The groupwise WM injury map (created using TFCE and FWE correction) is shown as a red (or white) overlay on structural T1 scans of two different "atlas" individuals, which, as expected, look similar. [Color figure can be viewed in the online issue, which is available at wileyonlinelibrary.com.]

assigned to each voxel essentially the number of standard deviation units the FA in the ALC group were from the LD group's FA. Any differences were not likely to be mediated by age as the two groups were equivalent in this variable; the *t*-map should reflect FA group differences related to alcohol dependence only.

2. The mean FA image (calculated using the LD only) in standardized space was coregistered to a particular "atlas" individual's FA map using SPM's 12-parameter nonaffine registration, and that same transformation was applied to the *t*-map created in Step 1.
3. The *t*-map was then intersected with that individual's "atlas" WM mask (also generated in SPM) to ensure the comparisons were only taken for voxels in that tissue class. The *t*-map was thresholded using a significance level of $P = 0.05$, resulting in a WM "injury" mask in the space of the "atlas" individual. Figure 2 shows thresholded ALC versus LD *t*-maps in the space of two different "atlas" individuals.
4. In the "atlas" tractogram, the tracts passing through the WM "injury" mask were recorded, along with the GM regions they connect.
5. LoCo was calculated for each GM region; it gives the percent of tracts connecting to that GM region that project through "injured" WM regions.

Steps 3–5 were repeated for each of the 14 "atlas" individuals and an average LoCo was calculated for each of the 90 GM regions. Scores closer to 1 indicate greater connectivity disruption for the particular GM region in the ALC group. The magnitude of injury was not considered as a continuous variable, but as all the injured voxels were above a certain level of significance, we assume a sort of "worst case" that can be captured with a binary mask.

Atrophy Calculation

For comparison with our LoCo score, another more conventional proxy for cortical involvement was measured: the volume of each GM region. We used the same process of GM parcellation into the 90 regions as described in the Image Processing section for the "atlas" data. The volume of each GM region was taken as the number of voxels assigned to each GM region out of the total number of voxels in all the cortical and subcortical regions (i.e., the volume is normalized to the individual's cortical plus subcortical volume). The atrophy measures were calculated both for ALC and LD and for the *t*-scores between the two groups subsequently computed. These *t*-scores, given in Supporting Information Table S2, can be viewed as proxies for cortical involvement in alcohol dependence, akin to LoCo.

Graph Theoretic Measures

In additional analyses, we compared differences between brain network summary statistics of ALC and LD groups. *T*-tests that compared the FA of the "atlas" group to the FA maps of the LD and ALC groups produced two *t*-maps. These *t*-maps were then coregistered to the individual "atlas" data and "injury" masks were produced as described in Step 3 of the Data section. Tracts going through those "injured" regions were completely removed, and the connectivity graph recalculated. The results of this process (outlined in Supporting Information Fig. S2) were

two groups of weighted connectivity matrices, one group that has been modified to incorporate the differences between LD and our "atlas" group and the other to incorporate the differences between ALC and the "atlas" group. Potential morphological changes due to age and image modality differences should be present in both comparisons; therefore, differences in graph metrics between these two pairings should be due solely to neurobiological differences between LD and ALC. We investigated differences in the following graph theoretical measures: characteristic path length (average shortest path length between nodes), efficiency (average of the inverse of shortest path length between nodes), average node eccentricity (average longest path length between connected nodes), radius (minimum node eccentricity), average node clustering coefficient (the degree to which a node's neighbors cluster together), average degree density (i.e., number of connections out of total amount possible between the 90 regions), and degree (number of connections per node).

Individual Subject Analysis

Deriving the LoCo score for all GM regions as described in the Data section consisted of comparing two groups' WM integrity maps and analyzing the resulting *t*-maps using hypothesis testing to create the WM injury mask. This method, however, did not give an individual LoCo for a particular participant. If the tissue differences in the ALC group are not spatially homogenous, the groupwise FA maps used in Graph Theoretic Measures section will not be as sensitive as comparing an ALC individual to a normal group. We therefore modified this process to yield individual LoCo scores by calculating the *z*-scores of an individual's FA map versus the LD group's mean and substituting it for the group comparison *t*-maps (see Supporting Information Fig. S3). Permutation and hypothesis testing is valid only for group comparisons, so to find areas of WM integrity loss on an individual level, we took voxels with *z*-scores above 1.96 and enforced a minimum cluster size of 5 to minimize noise effects. In this way, all of the ALC and LD individuals were assigned their own WM injury map and corresponding LoCo scores. Similarly, the individual's *z*-scores of GM volume were calculated by normalizing by the age-matched LD means.

Classification

A clinically useful metric accurately differentiates groups with a particular disease/condition from normal controls. Therefore, we compared those characteristics of the individual LoCo and volume scores in our study cohort by performing classification. Each participant was classified into LD and ALC groups using the remaining data (the jack-knife or leave-one-out process) via linear discriminant analysis [Krzanowski, 1988], as previously described in Raj et al. (2010). To test the quality of classification, we calculated the sensitivity (true positives divided by the sum of true positives and number of false negatives), specificity (true negatives out of the sum of true negatives and false positives) and classification rate (percent of correctly classified individuals).

As there are 90 values for each score corresponding to every ROI, it is desirable to perform dimensionality reduction on the data to reduce noise effects and improve classification. Singular value decomposition (SVD) was used to project the data into a smaller number of dimensions in order to maximize the data's variance. Several unsupervised reductions were performed and we chose the number of dimensions that demonstrated the maximum correct classification rate.

RESULTS

Group Analysis

Initially, the *t*-maps of the FA (ALC vs. LD) were corrected for multiple comparisons using the false discovery rate [FDR; Genovese et al., 2002]. However, due to the heterogeneity of the effect of alcohol dependence on the population and/or the subtlety of the differences, no voxels survived the FDR correction in the groupwise analysis (see Group versus Individual WM Injury Masks section for a detailed analysis). As cluster-level inference that makes use of the signal in local spatial neighborhood is generally found to be more sensitive than voxel-level inference, we implemented a method called threshold-free cluster enhancement [TFCE; Smith et al., 2009] in FSL (www.fmrib.ox.ac.uk/fsl). *P* value maps were created using the TFCE output image via (nonparametric) permutation testing and then corrected for multiple comparisons using the family wise error (FWE) approach, and thresholded for significance at $\alpha = 0.05$. The final groupwise WM injury map is shown in red in Figure 2, warped onto structural T1 scans of two different "atlas" individuals, which, as expected, look similar.

It must be noted here that hypothesis testing is only one way of identifying "injured" or compromised voxels, and in fact, the LoCo calculation does not require it. The problem of reliably finding injured WM voxels in individuals is challenging and may be done in a variety of ways. For instance, the WM injury map used to calculate LoCo may arise from an expert-drawn ROI, or manual fusion of multiple MRI modalities such as FLAIR and T2 to identify areas of WM hyperintensity or hypointensity. In fact, our approach can be modified to accommodate continuous (weighted) injury maps rather than binary masks. The benefit of a weighted mask is two-fold: it does not require that a hard decision as to the presence of injury be made at a voxel-wise level and it can also allow for more weight to be placed in highly injured areas. In such cases, hypothesis testing of WM injury maps is neither required nor desirable. Even when using hypothesis testing, inference is not being made directly on the voxels that are found to be different, but it is done on the cortical regions that have losses in connectivity due to "compromised" tissues. Hypothesis testing was implemented here to be more rigorous, but it can be argued

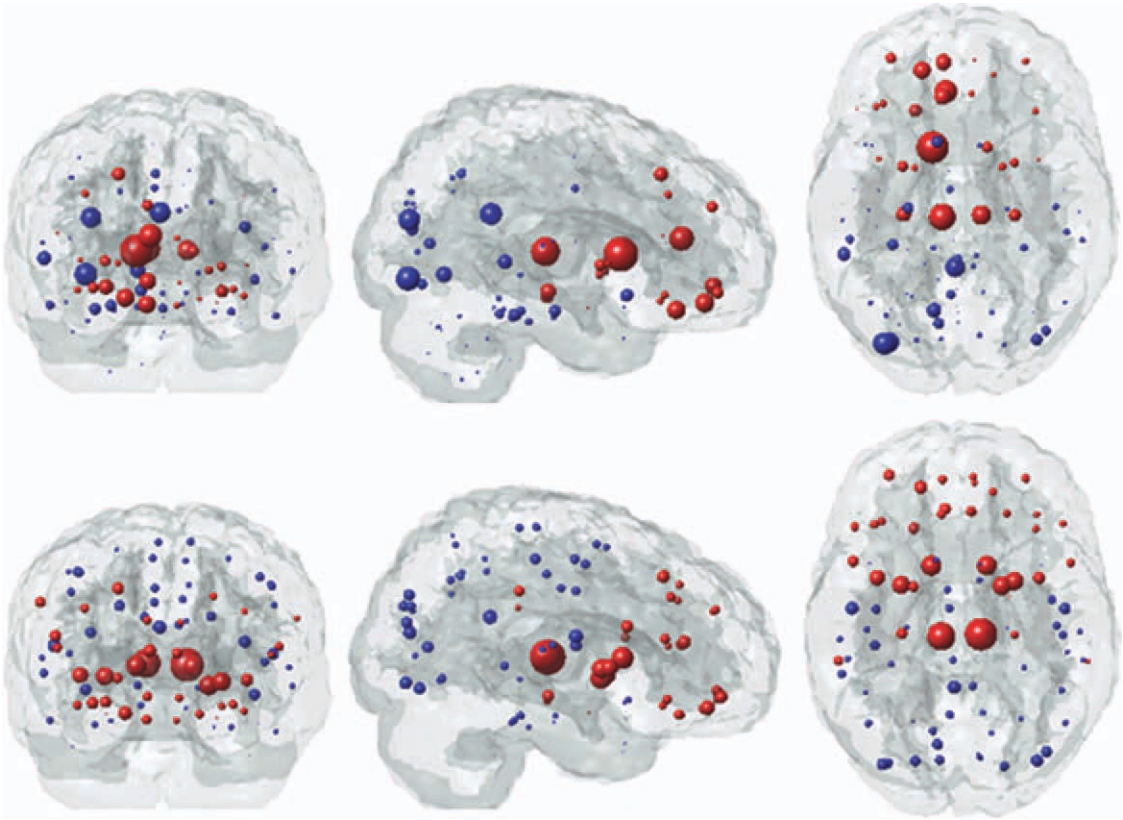

Figure 3.

LoCo scores correspond to the sizes of the circles that mark the center of each of the 90 GM ROIs (top row). The weights of the respective regions from the largest eigenvector, which was used in classification (bottom row). Red indicates BRS regions, non-BRS regions are shown in blue. [Color figure can be viewed in the online issue, which is available at wileyonlinelibrary.com.]

that LoCo scores resulting from WM "injury" maps calculated in other ways would still be valid.

LoCo and atrophy

Results of the whole brain analyses indicated that the bilateral thalamic structures, bilateral caudate, bilateral hippocampi, right putamen, right anterior and posterior cingulate, as well as right orbitofrontal and superior-frontal ROIs were among the top 25% of regions with the highest LoCo scores, that is, greatest relative connectivity loss (see Supporting Information Table S1 for a full list). The top row of Figure 3 visualizes the LoCo by plotting at the center of each region a circle the size of which is proportional to its LoCo; the BRS regions are shown in red, the non-BRS regions in blue. The right hemisphere (left in the figure) shows numerically higher LoCo values indicating greater connectivity disruption, in particular in the frontal cortex, subcortical, and temporooccipital regions.

ALC and LD showed no significant volume differences in any region after FDR correction or at $P < 0.05$ (uncorrected). Regions that tended to have smaller volumes in ALC ($P < 0.10$, uncorrected, corresponding to a one-tailed test) included frontal regions (bilateral superior frontal, right middle frontal, and bilateral superior medial frontal) as well as the right olfactory and left superior parietal ROIs. Some regions also tended to have larger volumes in ALC versus LD ($P < 0.10$, uncorrected, one-tail), including right middle orbital frontal, left frontal inferior operculum, bilateral middle and posterior cingulate, bilateral thalami, as well as bilateral supramarginal, left middle, and inferior temporal gyri.

BRS versus non-BRS. For ALC, the average LoCo of GM regions associated with the BRS (LoCo $= 0.027 \pm 0.024$, mean $\pm$ SD) was significantly larger than ($t = 2.18$, $P = 0.016$, one-tailed) the average LoCo of GM regions not in the BRS (LoCo $= 0.017 \pm 0.017$). The top row of Figure 4 shows the comparison of histograms of ALC LoCos, with the non-BRS regions on the right and the BRS regions on the left. For comparison, a *t*-test on the GM atrophy, as measured by *t*-scores for volumes between ALC and LD groups, in the BRS versus non-BRS revealed no significant

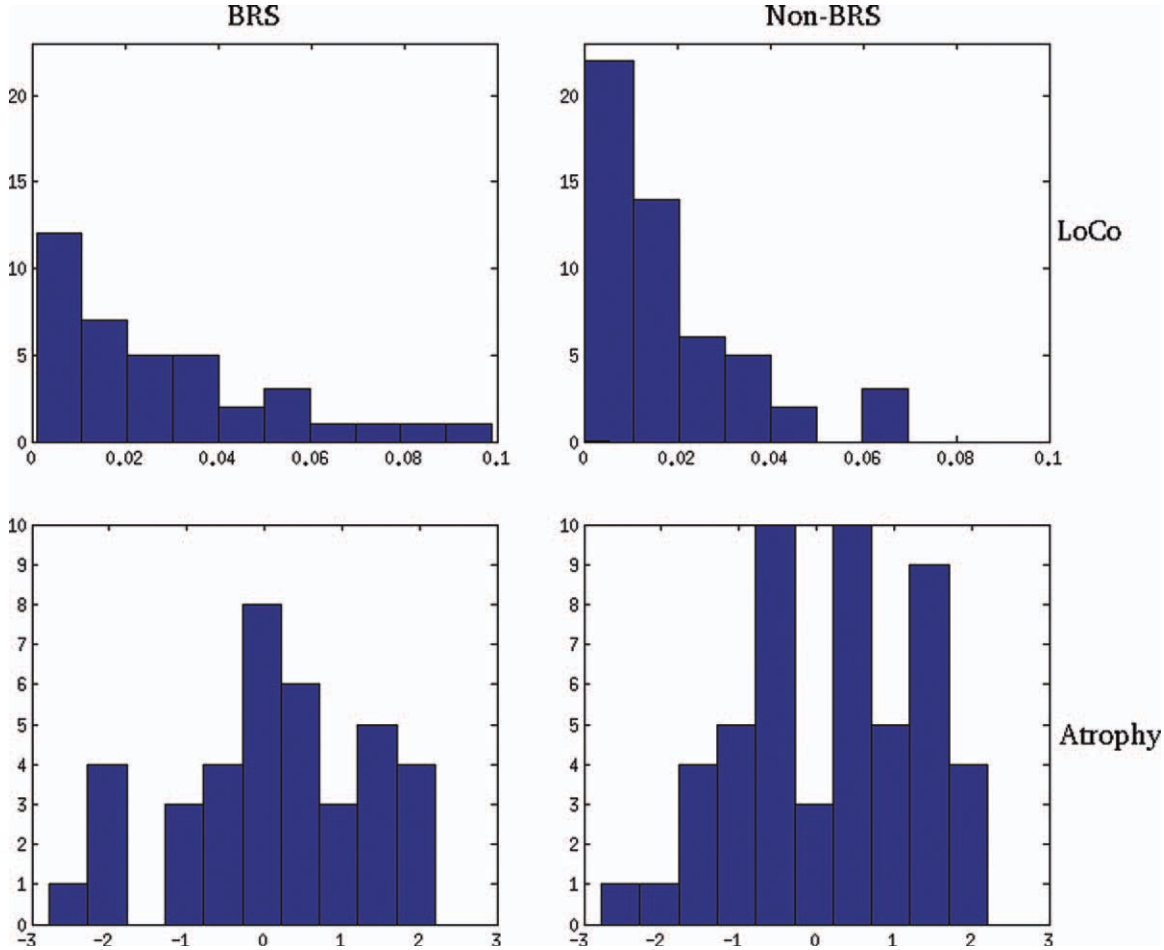

Figure 4.

Histograms of LoCo (top row) and GM atrophy (bottom row) for the ALC group in the BRS (left column) and non-BRS regions (right column). Negative values for GM atrophy correspond to volume loss. These values can be seen as a proxy for cortical involvement. These results are derived from the comparison of the BRS versus non-BRS at the level of the groupwise ALC LoCo scores, as described in Figure 1. [Color figure can be viewed in the online issue, which is available at wileyonlinelibrary.com.]

differences ($P = 0.58$, one-tailed), as shown in the second row of Figure 4.

Graph theoretical measures

The *t*-maps of the ALC versus "atlas" and LD versus "atlas" comparisons were generated using the same TFCE and FWE correction process as described for the group analysis previously described in this Section. No significant group differences were detected between ALC and LD for the overall network measures of characteristic path length, efficiency, average node eccentricity, radius, or average node clustering coefficient. Only the average degree density was significantly lower in ALC after FDR correction ($P = 0.006$). On an individual node basis, the degree was significantly lower in the ALC group (FDR corrected) in the following cortical regions: right middle frontal, right cuneus, and right superior temporal gyrus. There were no regions with an increase in degree or clustering coefficient (FDR corrected).

Individual Subject Analysis

BRS versus non-BRS: We tested the ALC individuals' LoCo scores for significant differences between the BRS and non-BRS. We averaged the LoCo scores for the BRS (0.036 ± 0.020) and non-BRS (0.025 ± 0.010) regions in each ALC individual and compared them using a paired *t*-test. The results shown in Supporting Information Figure S4 demonstrate that the BRS had significantly higher values than the non-BRS in the ALC population ($t = 5.26$, $P = 3.92 \times 10^{-6}$, one-tailed).

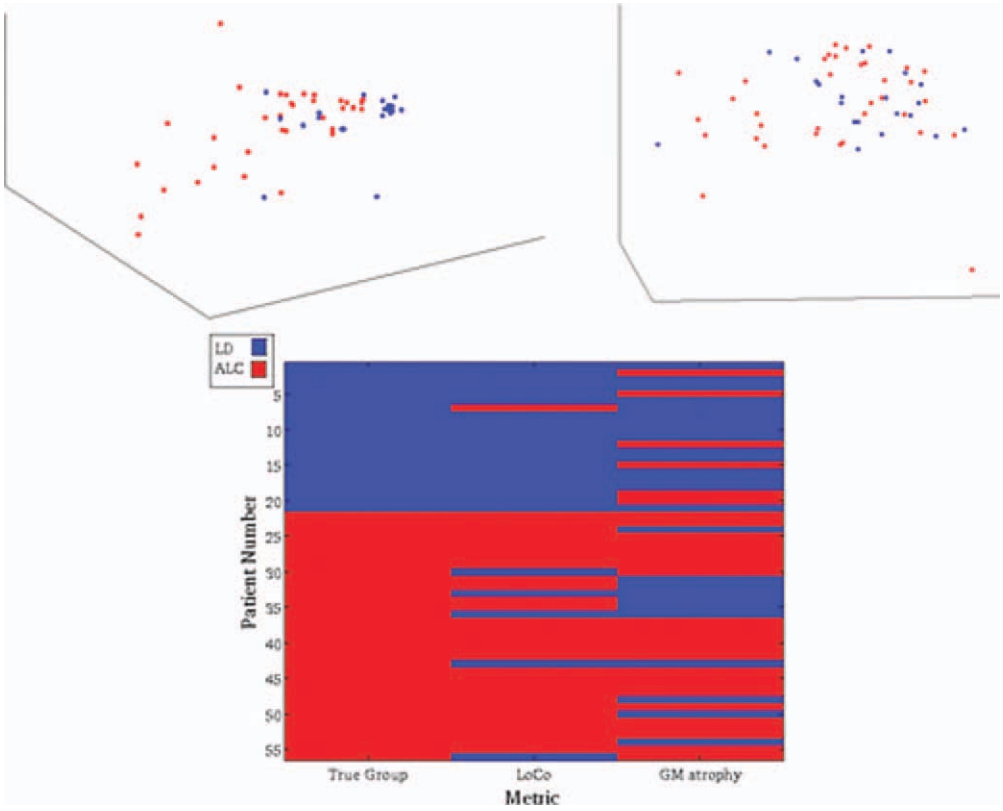

Figure 5.

The 3D scatter plots show the projection of the two metrics for each of the 56 ALC (black/red) and LD (gray/blue) participants onto their first three eigenvalues for LoCo (top left) and GM atrophy (top right). The higher degree of clustering is readily appreciated for LoCo values. In the bottom panel the classification results are shown for the ALC (black/red) and LD groups (gray/blue) using the two metrics, with the true grouping given in the first column. [Color figure can be viewed in the online issue, which is available at wileyonlinelibrary.com.]

Classification

We tested the power of the LoCo score to classify study participants into their respective diagnostic groups. Dimensionality reduction of the data was performed by projecting the data onto the first few eigenvectors in the SVD, as described in Classification section. Consistent with the LoCo group analyses above, we found that many regions given higher weight in the first eigenvector of the SVD of the LoCo were in fact in the BRS: bilateral thalami, caudate, putamen, pallidum, insula, and frontal cortex. The marker size in Figure 3 (bottom row) indicates the weight of that region, given in Supporting Information Table S3, in the first right eigenvector component of the LoCo score.

Figure 5 shows a scatter plot of the different metrics projected onto the first three eigenvectors of the SVD, with the LD participants in blue/gray and ALC participants in red/black. Note that even visually, the LoCo (top left) seems to separate the groups better than the GM volume measures (top right). In fact, the classification results for the two metrics, shown in the bottom panel of Figure 5, indicate that the LoCo demonstrates superiority, with overall correct classification rates of 89.3% versus 69.6% (Table II). In addition, we calculate the sensitivity and specificity and observe that the LoCo again had higher values at 85.7 and 95.2% versus 68.5 and 71.4%, respectively. The number of eigenvectors on which to project each metric—LoCo has 7 and volume has 37—were chosen to yield the highest classification rate. Even with about one-fifth of the number of eigenvectors, the LoCo achieves a better classification result than

TABLE II. The results of the classification using the two metrics and the number of eigenvectors that were used in the dimensionality reduction

Metric	# Eigen vectors	Specificity (%)	Sensitivity (%)	Classification rate (%)
LoCo	7	95.2	85.7	89.3
Z-score volume	37	71.4	69.6	69.6

volume. This speaks for the robustness of the newly derived LoCo measure.

Associations between imaging and drinking severity measures

To investigate associations among these measures with drinking severity, we projected each ALC's imaging metric onto its first eigenvector calculated using only the ALC group's image metrics. This provided a single number that summarized each metric by maximizing the variance over the ALC population and is essentially a weighted average over the brain regions, where the weights are exactly the values in the first eigenvector. As measures of drinking severity, we used the number of months of heavy drinking and the average number of drinks per month over lifetime, which, in previous work, have been shown to be most strongly related to neuroimaging and cognitive outcome measures. As this measure is dependent upon age, we calculate Spearman's partial correlation coefficient of the two imaging metrics with months of heavy drinking while controlling for the effects of age. Neither LoCo scores nor volumes were correlated with either measure of drinking severity (uncorrected or FDR corrected).

Group versus Individual WM Injury Masks

The groupwise FA comparison described in LoCo and Atrophy section revealed a relatively small volume of regions with WM injury in ALC. Here, we investigated whether this is related to spatial heterogeneity of the group differences or to their small magnitude. The difference in the FA (LD − ALC) and the standard deviation of the LD and ALC groups were calculated in voxels with FA greater than 0.1 (Supporting Information Fig. S5). The FA group difference is small compared to the FA standard deviations in both the LD and ALC group (with the ALC group having slightly higher standard deviation than the LD group). We then investigated the spatial heterogeneity of the individual WM injury masks by first taking the union of all the ALC individuals' WM injury masks. For each voxel in this union mask, we counted the number of times it was included in each of the 35 ALC individuals' WM injury masks. The results, shown in the histogram on the right in Supporting Information Figure S5, indicate that ∼85% of all of the voxels in the union WM injury mask were shared by five or less individuals' WM injury masks, indicating relatively little overlap in the ALC individuals' WM injury masks.

DISCUSSION AND CONCLUSIONS

In this study, we quantified relative changes of anatomical connections associated with alcohol dependence by using the location of WM differences between ALC and age-matched LD projected onto the whole-brain tractograms of young, healthy controls. LoCo, a recently defined predictive measure of cortical compromise, was employed [Kuceyeski and Raj, 2011; Kuceyeski et al., 2012]. This relative metric quantifies the loss of GM region connectivity measured by microstructural WM integrity loss. The LoCo in ALC was significantly higher (i.e., greater connectivity loss) across components of the BRS than across those not in the BRS. This suggests that the connectivity abnormalities demonstrated in this ALC cohort with 25 days of abstinence were most apparent in the BRS, a collection of unique and overlapping circuits critically involved in the development and maintenance of alcohol and other substance use disorders. Importantly, the LoCo findings indicated regionally specific abnormalities in WM connectivity among components of the frontal lobe, basal ganglia, thalami, and hippocampi. Our analysis, however, cannot distinguish between efferent and afferent connections between these nodes because tractography cannot provide directionality of fiber connections. The LoCo scores better discriminate ALC from LD than atrophy measures of the same GM nodes. This suggests the LoCo may provide more sensitive and specific information on the nature and extent of abnormalities in 25-day abstinent ALC than conventional measures of gross GM atrophy. We believe this may arise from either the higher sensitivity of diffusion MRI-based measures of WM integrity (which can detect small changes in microstructural integrity often before gross volume changes in the GM of the cortex or subcortical nuclei are apparent [Sullivan, 2007]), or from the fact that GM atrophy shows greater reversibility within a few weeks of abstinence [Gazdzinski et al., 2008, 2010], or both. Either way, this novel analysis is well suited for the assessment of brain structural abnormalities related to alcohol dependence—and, by extension, other substance dependence or neurological disorders—where gross measures of atrophy (i.e., brain volumes) may not be sufficiently sensitive.

Our finding that LoCo is higher in the BRS compared to non-BRS regions is consistent with previous studies implicating the BRS in the development and maintenance of alcohol use disorders [Durazzo et al., 2011; Koob and Volkow, 2010; Makris et al., 2008b; Volkow et al., 2011]. The WM changes in ALC individuals, while more prevalent in and among regions of the BRS, are both subtle and not spatially homogenous across the entire ALC population. The evidence of this is presented in Supporting Information Figure S5, which shows subtle group differences and little overlap in the ALC individuals' WM injury mask locations. Thus, both the inherent spatial variability of FA across the general population as well as the subtlety of FA differences contribute to the relatively small areas of groupwise significant differences. As a result, the LoCo scores derived from the groupwise comparison at the level of the FA maps show a weaker difference in the BRS versus non-BRS (Cohen's $d = 0.48$) than the LoCo scores derived from individual comparison of ALC FA maps against the LD group (Cohen's $d = 0.73$). The largely

negative graph theoretical analysis, in which we compared the ALC and LD group FA maps to the "atlas" FA maps, further supports this observation. In this study, volumetric measures did not indicate significant group differences in either BRS or non-BRS regions (after FDR correction), although several frontal GM volumes tended to be smaller in the ALC cohort. Previous larger studies in alcohol-dependent populations have shown significant volume differences, for example, Harper et al. (2005) and Gazdzinski et al. (2005). In a larger cohort and using FreeSurfer methodology [Durazzo et al., 2011], we observed smaller BRS volumes in 7-day-abstinent ALC versus LD, in agreement with Makris et al. (2008b). Lower statistical power in this study may be related to smaller sample sizes, the difference in the tools used to measure volume (i.e., FreeSurfer vs. SPM here), and/or the presence of significant brain volume recovery within the 3–4 weeks of abstinence [Gazdzinski et al., 2008, 2010] presumably demonstrated by the ALC group.

We draw particular attention to the fact that the first principal component of the individuals' LoCo scores generally coincides with the BRS (Fig. 3, bottom row), an independent confirmation of the relevance of the BRS in distinguishing ALC from LD. To our knowledge, this is a unique finding, which simply implies that if one looks for the linear combination of LoCo scores in various brain regions that maximizes the LoCo variance across all cohort groups, the LoCo of the BRS regions are given higher weights. This suggests that the morphological abnormalities associated with alcohol dependence, whether due to microstructural or volumetric changes in the connecting WM fibers, may be manifested to a greater extent in the BRS. The loss in WM integrity measures like FA may also reflect a demyelination [Gadzinski et al., 2010] or tissue degradation due to oxidative stress.

Oxidative stress is proposed as a major pathophysiologic mechanism that contributes to structural and biochemical abnormalities in alcohol use disorders, including neuronal injury [Alfonso-Loeches and Guerri, 2011; Crews and Nixon, 2009]. It results from increased levels of reactive oxygen and nitrogen radical species and other oxidizing agents from exposure to, and metabolism of, excessive alcohol [Alfonso-Loeches and Guerri, 2011; Crews and Nixon, 2009]. Radical species/oxidizing agents directly promote oxidative damage to membrane lipids, proteins, carbohydrates, and DNA. The WM in the anterior frontal and mesial temporal lobes, much of which connects nodes of the BRS, are particularly vulnerable to oxidative stress [Bartzokis, 2004; Kochunov et al., 2007; Wang and Michaelis, 2010].

We did not find associations of LoCo measures with alcohol consumption in this study. This may indicate that the patterns demonstrated by ALC were present before the onset of hazardous drinking [Fineberg et al., 2010; Tessner et al., 2010]. If the observed connectivity loss in this ALC cohort is indeed premorbid, then the greater LoCo in the BRS may serve as a specific risk factor for the development of alcohol use disorders. It is also possible that the injury patterns in the ALC cohort are a function of concurrent environmental factors and other comorbid conditions not assessed in this study [Durazzo and Meyerhoff, 2007; Meyerhoff and Durazzo, 2008; Meyerhoff et al., 2011]. It is still an open question as to whether anatomical brain changes in alcohol dependence are premorbid, but the longitudinal recovery of FA in abstinent individuals [Gadzinski et al., 2010] seems to suggest that changes in the WM are indeed associated with alcohol consumption and that abstinence may promote recovery of damaged tracts. Longitudinal studies will be needed to determine if the LoCo scores that depend on FA can also recover. Overall, however, this study presents a new sensitive marker of anatomical connectivity loss between functionally relevant GM nodes in ALC. Our findings are complementary to and consistent with our other neuroimaging work in ALC comprising many of these study participants, which have revealed the greatest and most significant brain effects in components of the BRS.

Limitations and Future Work

It is an ongoing debate whether observed changes in brain morphology or microstructural integrity are a consequence of excessive alcohol consumption, or whether they represent intrinsic malformations, which predispose to risky and/or addictive behavior. This issue cannot be addressed using the proposed analysis, which is a major limitation that this study shares with most previous cross-sectional studies in adults. Longitudinal studies can assess if abnormalities resolve with abstinence and further research can evaluate genetic predispositions.

The lack of significant volume changes in this study is in disagreement with a previous study in a similar alcohol-dependent cohort [Makris et al., 2008a, 2008b] that study used a larger cohort and an in-house method to calculate regional tissue volumes. We will apply the LoCo analyses in larger cohorts when they become available and possibly use more sensitive measures of volume and/or cortical thickness, such as FreeSurfer or CIVET [Ad-Dab'bagh et al., 2006].

Chronic cigarette smoking, although shown to affect brain volumes and DTI metrics in alcohol dependence and nonalcohol-dependent cohorts [Durazzo and Meyerhoff, 2007; Gazdzinski et al., 2005, 2008; Gons et al., 2011; Zhang et al., 2011], was not specifically considered in these analyses. Here, 66% of our ALC cohort and 57% of our LD cohort were chronic cigarette smokers. Although the group prevalence of chronic smoking was not significantly different, we cannot exclude that the observed effects reported in this study are solely associated with chronic heavy drinking. Smoking was not included in the design of the study as it would make the groups smaller and consequently diminish potential differences. Future studies in a larger cohort will address the degree to which either

dependence contributes to the observed structural abnormalities in ALC. It must be noted that there is a relative lack of female participants in these veteran ALC and gender-matched LD groups, so any gender-related differences would not affect this analysis. Future studies will attempt to recruit more women for both groups.

A well-known issue in tractography is the difficulty elucidating underlying structure in areas of crossing, kissing, or fanning fibers. Also, as in any methodology that relies on tractography, long-distance fiber connections could be systematically ignored. We hypothesize, however, that the number of long-range connections that are overlooked is small in comparison to the number of medium and short-range fibers that are included in the LoCo score.

The LD group was used to create the standard-space FA template, which could cause registration errors when normalizing the ALC group if anatomical differences exist between the two groups - especially in subcortical areas that include many regions in the BRS. However, as we showed in the Results section, there were no significant differences in groupwise cortical and subcortical volumes, so it can be assumed that any coregistration errors would be small. In addition, we hand-checked each ALC image for no visible spatial discrepancies with the LD FA template. Even if there were problems with coregistration in the subcortical areas that were not visible, the result would be a noisier LoCo score in these areas, not a systematic increase or decrease of its value.

In conclusion, the new LoCo metric is shown to be sensitive to relative anatomical connectivity losses in alcohol dependent compared to LD individuals. LoCo in alcohol dependence reveals structural connectivity disruptions that are specific to regions of the BRS. In contrast to Alzheimer's disease and Frontotemporal dementia [Kuceyeski et al., 2012], we found the LoCo score of GM regions in our abstinent ALC not correlated with the corresponding GM volumes. As such, this new measure may display high specificity and sensitivity to brain structural network disruptions in alcohol dependence not captured by conventional atrophy measures.

ACKNOWLEDGMENT

The authors thank the Brain Trauma Foundation for sharing the image data from the young healthy normal population.

REFERENCES

Ad-Dab'bagh Y, Einarson D, Lyttelton O, Muehlboeck JS, Mok K, Ivanov O, Vincent RD, Lepage C, Lerch J, Fombonne E, Evans AC (2006): The CIVET image-processing environment: A fully automated comprehensive pipeline for anatomical neuorimaging research. Proceedings of the 12th Annual Meeting of the Organization for Human Brain Mapping (OHBM), p 2266.

Alemán-Gómez Y, Melie-García L, Valdés-Hernandez P (2005): IBASPM: Toolbox for automatic parcellation of brain structures. Presented at the 12th Annual Meeting of the Organization for Human Brain Mapping, Florence, Italy.

Alfonso-Loeches S, Guerri C (2011): Molecular and behavioral aspects of the actions of alcohol on the adult and developing brain. Crit Rev Clin Lab Sci 48:19–47.

Aralasmak A, Ulmer JL, Kocak M, Salvan CV, Hillis AE, Yousem DM (2006): Association, commissural, and projection pathways and their functional deficit reported in literature. J Comput Assist Tomogr 30:695–715.

Bartzokis G (2004): Quadratic trajectories of brain myelin content: Unifying construct for neuropsychiatric disorders. Neurobiol Aging 25:49–62.

Bendlin BB, Ries ML, Canu E, Sodhi A, Lazar M, Alexander A, Carlsson C, Sager M, Asthana S, Johnson SC (2010): White matter is altered with parental family history of Alzheimer's disease. Alzheimers Dement 6:9.

Cardenas VA, Studholme C, Gazdzinski S, Durazzo TC, Meyerhoff DJ (2007): Deformation-based morphometry of brain changes in alcohol dependence and abstinence. NeuroImage 34:879–887.

Cardenas VA, Durazzo TC, Gazdzinski S, Mon A, Studholme C, Meyerhoff DJ (2011): Brain morphology at entry into treatment for alcohol dependence is related to relapse propensity. Biol Psychiatry 70:561–567.

Crews FT, Nixon K (2009): Mechanisms of neurodegeneration and regeneration in alcoholism. Alcohol 44:115–127.

Durazzo TC, Gazdzinski S, Banys P, Meyerhoff DJ (2004): Cigarette smoking exacerbates chronic alcohol-induced brain damage: A preliminary metabolite imaging study. Alcohol Clin Exp Res 28:1849–1860.

Durazzo TC, Meyerhoff DJ (2007): Neurobiological and neurocognitive effects of chronic cigarette smoking and alcoholism. Front Biosci 12:4079–4100.

Durazzo TC, Pathak V, Gazdzinski S, Mon A, Meyerhoff DJ (2010): Metabolite levels in the brain reward pathway discriminate those who remain abstinent from those who resume hazardous alcohol consumption after treatment for alcohol dependence. J Stud Alcohol Drug 71:278–289.

Durazzo TC, Tosun D, Buckley S, Gazdzinski S, Mon A, Fryer SL, Meyerhoff DJ (2011): Cortical thickness, surface area, and volume of the brain reward system in alcohol dependence: Relationships to relapse and extended abstinence. Alcohol Clin Exp Res 35:1187–1200.

Durazzo TC, Mon A, Gazdzinski S, Meyerhoff DJ (2011): Chronic cigarette smoking in alcohol dependence: Associations with cortical thickness and N-acetylaspartate levels in the extended brain reward system. Addict Biol. doi:10.1111/j.1369–1600.2011.00407.x.

Filley CM (2005): White matter and behavioral neurology. Ann N Y Acad Sci 1064:162–183.

Fineberg NA, Potenza MN, Chamberlain SR, Berlin HA, Menzies L, Bechara A, Sahakian BJ, Robbins TW, Bullmore ET, Hollander E (2010): Probing compulsive and impulsive behaviors, from animal models to endophenotypes: A narrative review. Neuropsychopharmacology 35:591–604.

First M, Spitzer R, Gibbon M, Williams J (1998): Structured Clinical Interview for DSM-IV Axis I Disorders—Patient Edition (SCID-I/P, Version 2.0:8/98 revision). New York: Biometrics Research Department.

Friston K, Ashburner J, Kiebel S, Nichols T, Penny W. 2007. Statistical Parametric Mapping: The Analysis of Functional Brain Images. Elsevier.

Gazdzinski S, Durazzo TC, Studholme C, Song E, Banys P, Meyerhoff DJ (2005): Quantitative brain MRI in alcohol dependence: Prelimi-

nary evidence for effects of concurrent chronic cigarette smoking on regional brain volumes. Alcohol Clin Exp Res 29:1484–1495.

Gazdzinski S, Durazzo TC, Mon A, Yeh P-H, Meyerhoff DJ (2010): Cerebral white matter recovery in abstinent alcoholics—A multimodality magnetic resonance study. Brain 133:1043–1053.

Gazdzinski S, Durazzo TC, Yeh P-H, Hardin D, Banys P, Meyerhoff DJ (2008): Chronic cigarette smoking modulates injury and short-term recovery of the medial temporal lobe in alcoholics. Psychiatry Res 162:133–145.

Genovese C, Wasserman L (2002): Operating characteristics and extensions of the false discovery rate procedure. J R Stat Soc Ser B 64:499–517.

George O, Koob GF (2010): Individual differences in prefrontal cortex function and the transition from drug use to drug dependence. Neurosci Biobehav Rev 35:232–247.

Gold BT, Powell DK, Andersen AH, Smith CD (2010): Alterations in multiple measures of white matter integrity in normal women at high risk for Alzheimer's disease. NeuroImage 52:1487–1494.

Griswold MA, Jakob PM, Heidemann RM, Nittka M, Jellus V, Wang J, Kiefer B, Haase A (2002): Generalized autocalibrating partially parallel acquisitions (GRAPPA). Magn Reson Med 47:1202–1210.

Harper C, Matsumoto I, Pfefferbaum A, Adalsteinsson E, Sullivan EV, Lewohl J, Dodd P, Taylor M, Fein G, Landman B (2005): The pathophysiology of brain shrinkage in alcoholics structural and molecular changes and clinical implications. Alcohol: Clin Exp Res 29:1106–1115.

Heinz A, Beck A, Grüsser SM, Grace AA, Wrase J (2009): Identifying the neural circuitry of alcohol craving and relapse vulnerability. Addict Biol 14:108–118.

Kochunov P, Thompson PM, Lancaster JL, Bartzokis G, Smith S, Coyle T, Royall DR, Laird A, Fox PT (2007): Relationship between white matter fractional anisotropy and other indices of cerebral health in normal aging: Tract-based spatial statistics study of aging. Neuroimage 35:478–487.

Kolb B, Whishaw I. 2009. Fundamentals of Human Neuropsychology. Worth Publishers.

Koob GF, Volkow ND (2010): Neurocircuitry of addiction. Neuropsychopharmacology 35:217–238.

Krzanowski WJ. 1988. Principles of Multivariate Analysis: A User's Perspective. Clarendon Press.

Kuceyeski A, Maruta J, Niogi SN, Ghajar J, Raj A (2011): The generation and validation of white matter connectivity importance maps. NeuroImage 58:109–121.

Kuceyeski A, Raj A (2011): Investigating correlations of cortical atrophy and white matter integrity loss in Alzheimer's subjects using connectivity information. Alzheimer's Association International Conference on Alzheimer's Disease, Paris, France, p 16242.

Kuceyeski A, Zhang Y, Raj A (2012): Linking white matter connectivity integrity loss to associated cortical regions using structural connectivity information in Alzheimer's disease and fronto-temporal dementia: The Loss in Connectivity (LoCo) score. NeuroImage 61:1311–1323.

Lo C-Y, Wang P-N, Chou K-H, Wang J, He Y, Lin C-P (2010): Diffusion tensor tractography reveals abnormal topological organization in structural cortical networks in Alzheimer's disease. J Neurosci 30:16876–16885.

Makris N, Gasic GP, Kennedy DN, Hodge SM, Kaiser JR, Lee MJ, Kim BW, Blood AJ, Evins AE, Seidman LJ, Iosifescu DV, Lee S, Baxter C, Perlis RH, Smoller JW, Fava M, Breiter HC (2008a): Cortical thickness abnormalities in cocaine addiction—A reflection of both drug use and a pre-existing disposition to drug abuse? Neuron 60:174–188.

Makris N, Oscar-Berman M, Jaffin SK, Hodge SM, Kennedy DN, Caviness VS, Marinkovic K, Breiter HC, Gasic GP, Harris GJ (2008b): Decreased volume of the brain reward system in alcoholism. Biol Psychiatry 64:192–202.

Meyerhoff DJ, Durazzo TC, Ende G (2011): Chronic alcohol consumption, abstinence and relapse: Brain proton magnetic resonance spectroscopy studies in animals and humans. Curr Top Behav Neurosci.

Meyerhoff DJ, Durazzo TC (2008): Proton magnetic resonance spectroscopy in alcohol use disorders: A potential new endophenotype? Alcohol Clin Exp Res 32:1146–1158.

Pfefferbaum A, Adalsteinsson E, Sullivan EV (2006): Dysmorphology and microstructural degradation of the corpus callosum: Interaction of age and alcoholism. Neurobiol Aging 27:994–1009.

Pfefferbaum A, Rosenbloom MJ, Adalsteinsson E, Sullivan EV (2007): Diffusion tensor imaging with quantitative fibre tracking in HIV infection and alcoholism comorbidity: Synergistic white matter damage. Brain 130:48–64.

Pfefferbaum A, Sullivan EV (2005): Disruption of brain white matter microstructure by excessive intracellular and extracellular fluid in alcoholism: Evidence from diffusion tensor imaging. Neuropsychopharmacology 30:423–432.

Raj A, Mueller SG, Young K, Laxer KD, Weiner M (2010): Network-level analysis of cortical thickness of the epileptic brain. NeuroImage 52:1302–1313.

Rando K, Hong K-I, Bhagwagar Z, Li C-SR, Bergquist K, Guarnaccia J, Sinha R (2011): Association of frontal and posterior cortical gray matter volume with time to alcohol relapse: A prospective study. Am J Psychiatry 168:183–192.

Schmahmann JD, Pandya DN, Wang R, Dai G, D'Arceuil HE, Crespigny AJ de, Wedeen VJ (2007): Association fibre pathways of the brain: Parallel observations from diffusion spectrum imaging and autoradiography. Brain 130:630–653.

Skinner HA, Sheu WJ (1982): Reliability of alcohol use indices. The lifetime drinking history and the MAST. J Stud Alcohol 43:1157–1170.

Smith CD, Chebrolu H, Andersen AH, Powell DA, Lovell MA, Xiong S, Gold BT (2010): White matter diffusion alterations in normal women at risk of Alzheimer's disease. Neurobiol Aging 31:1122–1131.

Smith SM and Nichols TE (2009): Threshold-free cluster enhancement: Addressing problems of smoothing, threshold dependence and localisation in cluster inference. NeuroImage 44:83–98.

Sobell LC, Sobell MB, Riley DM, Schuller R, Pavan DS, Cancilla A, Klajner F, Leo GI (1988): The reliability of alcohol abusers' self-reports of drinking and life events that occurred in the distant past. J Stud Alcohol 49:225–232.

Sobell LC, Sobell MB (1990): Self-report issues in alcohol abuse: State of the art and future directions. Behav Assess 12:91–106.

Sullivan EV (2007): Alcohol and drug dependence: Brain mechanisms and behavioral impact. Neuropsychol Rev 17:235–238.

Sullivan EV, Rohlfing T, Pfefferbaum A (2010): Quantitative fiber tracking of lateral and interhemispheric white matter systems in normal aging: Relations to timed performance. Neurobiol Aging 31:464–481.

Sullivan EV, Pfefferbaum A (2005): Neurocircuitry in alcoholism: A substrate of disruption and repair. Psychopharmacology 180:583–594.

Tessner KD, Hill SY (2010): Neural circuitry associated with risk for alcohol use disorders. Neuropsychol Rev 20:1–20.

Volkow ND, Wang G-J, Fowler JS, Tomasi D, Telang F, Baler R (2010): Addiction: Decreased reward sensitivity and increased expectation sensitivity conspire to overwhelm the brain's control circuit. Bioessays 32:748–755.

Volkow ND, Wang G-J, Fowler JS, Tomasi D, Telang F (2011): Quantification of behavior sackler colloquium: Addiction: Beyond dopamine reward circuitry. Proc Natl Acad Sci USA 108:15037–15042.

Wang X, E.K. Michaelis (2010): Selective neuronal vulnerability to oxidative stress in the brain. Front Aging Neurosci 2:12.

Wen W, Zhu W, He Y, Kochan NA, Reppermund S, Slavin MJ, Brodaty H, Crawford J, Xia A, Sachdev P (2011): Discrete neuroanatomical networks are associated with specific cognitive abilities in old age. J Neurosci 31:1204–1212.

Yeh P-H, Simpson K, Durazzo TC, Gazdzinski S, Meyerhoff DJ (2009): Tract-based spatial statistics (TBSS) of diffusion tensor imaging data in alcohol dependence: Abnormalities of the motivational neurocircuitry. Psychiatry Res 173:22–30.

Zalesky A, Fornito A, Bullmore ET (2010): Network-based statistic: Identifying differences in brain networks. NeuroImage 53:1197–1207.

Zhang X, Salmeron BJ, Ross TJ, Geng X, Yang Y, Stein EA (2011): Factors underlying prefrontal and insula structural alterations in smokers. NeuroImage 54:42–48.